NANO · MICRO small
www.small-journal.com

Highly Dispersed Copper Nanoparticles Supported on Activated Carbon as an Efficient Catalyst for Selective Reduction of Vanillin

Ruoyu Fan, Chun Chen, Miaomiao Han, Wanbing Gong, Haimin Zhang, Yunxia Zhang, Huijun Zhao,* and Guozhong Wang**

Highly dispersed copper nanoparticles (Cu NPs) supported on activated carbon (AC) are effectively synthesized by one-pot carbothermal method at temperature range of 400–700 °C. The X-ray diffraction, transmission electron microscopy, X-ray photoelectron spectroscopy, and Brunauer–Emmett–Teller analysis reveal that Cu NPs with diameters of 20–30 nm are evenly anchored in carbon matrix. The 15 wt%-Cu/AC-600 catalyst (derived at 600 °C) exhibits best bifunctional catalysis of aqueous-phase hydrodeoxygenation (HDO) and organic-phase transfer-hydrogenation reaction (THR) to selectively transform vanillin to 2-methoxy-4-methylphenol (MMP). In HDO of vanillin, the as-prepared catalyst achieves a 99.9% vanillin conversion and 93.2% MMP selectivity under 120 °C, 2.0 MPa H_2 within 5 h. Meanwhile, near-quantitative vanillin conversion and 99.1% MMP selectivity are also obtained under 180 °C within 5 h in THR of vanillin by using 2-propanol as hydrogen donor. The transforming pathways of vanillin are also proposed: vanillin is transformed into MMP via intermediate of 4-hydroxymethyl-2-methoxyphenol in HDO case and by direct hydrogenolysis of vanillin in THR course. More importantly, the activity and the selectivity do not change after 5 cycles, indicating the catalyst has excellent stability. The Cu-based catalyst is relatively cheap and preparation method is facile, green, and easy scale-up, thus achieving a low-cost transformation of biomass to bio-oils and chemicals.

1. Introduction

The conversion of biomass into fuels and chemicals is an effective way to reduce the world dependence on fossil resources and environment pollution simultaneously.[1,2] As one of the three major components in lignocellulosic biomass, lignin is the only renewable source that can be firsthand applied to produce aromatic compounds, like bio-oil.[3] However, these products cannot be directly used because of high oxygen content.[4] Catalytic hydrodeoxygenation (HDO), which involves hydrogenation of unsaturated functional groups like C=C bonds followed by the hydrogenolysis of C—O bonds, has been deemed to be one of the most important and effective upgrading strategies to reduce the oxygen content.[5–7]

As an important aromatic monomer in lignin, vanillin can be selectively transformed into 2-methoxy-4-methylphenol (MMP), which has been widely used as fragrances or the intermediates of drugs and fragrances, by the catalytic HDO over various heterogeneous catalysts.[8] Among them, noble metal-based catalysts are predominant because of their high activity, such as Au/carbon nanotubes,[9] Ru nanoclusters,[10] Ru/carbon nanotube,[11] hollow Pd/metal organic framework nanosphere,[12] Pd/single-walled carbon nanotube-SiO_2,[13] and Pd/MSMF (MSMF: superhydrophilic mesoporous sulfonated melamine-formaldehyde resin),[14] Pd/SO_3H-MIL-101(Cr), etc.[15] It could be easily found that cumbersome synthetic strategies or complicated supports were usually unavoidable for construction these high active noble metal-based catalyst.[16–22] In addition, using noble metal-based catalysts are prone to fall into the dilemma of low selectivity to MMP, yielding the mixture of MMP and 4-hydroxymethyl-2-methoxyphenol (HMP).[13] More seriously, noble metal-based catalysts are usually limited to practical application by coke formation, easy deactivation, as well as their low reserves and high cost. On these basis, there is a pressing need for developing highly active, selective and steady non-noble metal-based catalysts with the prospects in practical application.[23,24]

Recently, several non-noble metal catalysts have been developed to catalyze the reaction of HDO, such as Co, Ni, and Cu

---

R. Fan, Dr. C. Chen, Dr. M. Han, W. Gong, Prof. H. Zhang,
Prof. Y. Zhang, Prof. H. Zhao, Prof. G. Wang
Key Laboratory of Materials Physics
Centre for Environmental and Energy Nanomaterials
Anhui Key Laboratory of Nanomaterials and Nanotechnology
CAS Center for Excellence in Nanoscience
Institute of Solid State Physics
Chinese Academy of Sciences
Hefei, Anhui 230031, China
E-mail: chenchun2013@issp.ac.cn; h.zhao@griffith.edu.au;
gzhwang@issp.ac.cn

R. Fan, W. Gong
Science Island Branch of Graduate School
University of Science and Technology of China
Hefei, Anhui 230026, China

Prof. H. Zhao
Centre for Clean Environment and Energy
Gold Coast Campus
Griffith University
Queensland 4222, Australia

The ORCID identification number(s) for the author(s) of this article can be found under https://doi.org/10.1002/smll.201801953.

DOI: 10.1002/smll.201801953

catalysts, which are preferable than noble metal catalysts for the potentials of commercial application and economy. Xia et al. reported HDO of vanillin to MMP in liquid-phase can be achieved with a selectivity of 64.6% over a highly dispersed Ni/nitrogen-doped carbon black catalyst.[25] Tsang et al. reported an efficient catalyst (Co-MoS_2), which exhibits high catalytic performance in HDO of 4-methylphenol under mild reaction conditions.[26] Chen and co-workers reported well-dispersed Mo_2C nanoparticles supported on activated carbon, exhibiting excellent catalytic activity in HDO of vanillin but poor selectivity for target products under mild reaction conditions.[27] Although these catalysts have demonstrated identified activity of HDO, a great challenge is upgrading the selectivity to the target product. Among various types of non-noble catalysts, Cu-based heterogeneous catalyst has a unique advantage for chemoselective HDO of aromatic or heterocyclic aldehydes in view of its moderate activity and specific adsorption manner. It has reported that the hydrogenation of aromatic or heterocyclic aldehydes over Cu-based catalyst usually following a η^1(O)-aldehyde (perpendicular) configuration, in which the O atom of aldehyde group is contacted with Cu to form η^1(O)- species and at the same time the aromatic or heterocyclic ring is repelled away from the catalyst surface to remain largely unaffected.[28] By this adsorption manner, the reaction site can be confined to the aldehyde group, and thus achieving chemoselective HDO of aromatic or heterocyclic aldehydes.[29] Therefore, Cu is the desired candidate as active metal element for selective HDO of vanillin toward MMP. Compared with Ni- or other metallic-based catalyst, the Cu-based catalyst possesses moderate catalytic activity and has low tendency to catalyze aromatic or heterocyclic ring which can prevent excessive HDO of reactant to some by-products, thus improving its selectivity.[30] Up to now, Cu-based catalysts have been widely used for the HDO reaction, such as Cu/SiO_2,[28] Cu-HZSM-5,[31] CuMgAl,[32] CuZnAl,[32] Cu/MgO,[33] Co-Cu/SBA-15,[34] and $Cu_{30}Cr_{10}/\gamma$-Al_2O_3.[35] Lomate et al. have studied selective hydrogenation of levulinic acid to γ-valerolactone over Cu-SiO_2 catalysts.[36] Nagaraja et al. reported a highly efficient Cu/MgO catalyst for vapour phase hydrogenation of furfural to furfuryl alcohol, in which high conversion of furfural (98.0%) and high selectivity toward furfuryl alcohol (98.0%) were achieved.[33] Recently, Petitjean et al prepared a Cu-PMO (PMO: porous metal oxide) catalyst and applied it into HDO of vanillin, which gave a 100% conversion and 90% MMP selectivity under 180 °C and 4.0 MPa H_2 pressure within 18 h.[37] Moreover, the corresponding catalyst could be extended to catalytic reduction of other unsaturated compounds. However, more or less, these Cu-based catalysts had some imperfections, such as complicated or multisteps synthetic method, harsh reaction conditions and easy deactivation. In addition, they could only be used in conventional catalytic hydrogenation process with the assistance of high pressure H_2, which would induce many drawbacks, such as high cost, low solubility, complex reactor design, and high requirements for storage, transportation, and safety. Although catalytic conversion of vanillin were also achieved without using molecular H_2 by transfer hydrogenation reaction (THR), the catalysts were confined to noble metal-based materials, such as $Pd_{50}Ag_{50}/Fe_3O_4$/nitrogen-doped reduced graphene oxide,[17] Ag-Pd@g-C_3N_4,[20] and Pd/nitrogen-enriched highly mesoporous carbon catalysts.[38] Therefore, we aim at developing a bifunctional non-noble metal-based catalyst, which can not only display high activity in direct HDO of vanillin by molecular H_2, but also can efficiently convert vanillin toward MMP with H_2-free via a THR route.

Here, metallic Cu was selected as the active component. And for constructing of highly active heterogeneous Cu-based catalyst, an eligible support with the properties of high surface, good thermal stability and economy is necessary, like carbon materials. Furthermore, the use of carbon as support can also reduce the formation of coke, which is difficult to avoid in other supports, like Al_2O_3, in the course of HDO reactions. Considering that there is a strong interaction between metal ions and carbon at high temperature (reducing property of active carbon), a carbon supported Cu catalyst (Cu/AC) was constructed by carbothermal method, in which the Cu ions was reduced by carbon and the formed Cu nanoparticles (NPs) were in situ anchored on the carbon. In this process, the carbon was acted as the reductant, stabilizer, dispersant, as well as the support for Cu NPs. The Cu/AC catalyst was applied in the processes of HDO and THR of vanillin toward MMP under a moderate reaction condition, and their activities and selectivities were also evaluated and correlated with the structures of prepared material.

2. Results and Discussion

2.1. Screen for the Cu/AC-600 Catalyst

First, we screened the structure and morphology of 15 wt%-Cu/AC-600 catalyst and the corresponding characterization results are shown in **Figure 1**. The powder X-ray diffraction (XRD) patterns of the as-obtained sample displays a broad peak located at $2\theta = 23.0°$, which could be attributed to the characteristic peak of amorphous carbon (Figure 1a). And another three characteristic diffraction peaks at 2θ values of 43.3°, 50.5°, 74.2° are corresponded to (111), (200), (220) planes of metallic Cu (JCPDS 01-070-3039), suggesting the Cu precursors are effectively reduced into metallic Cu by the carbothermal method. The average size of the Cu NPs is 32.1 nm calculated by Debye–Scherrer formula. The specific surface area of Brunauer–Emmett–Teller (S_{BET}) and pore volume (V_{pore}) of the prepared sample were also determined by the N_2 physisorption technique (Figure 1b), which displays microporous solids (pore size of 1.4 nm) and high surface area of 822 $m^2\ g^{-1}$, being benefit for catalytic conversion of vanillin. In addition, the morphologies and metal dispersions of 15 wt%-Cu/AC-600 catalyst were also characterized by transmission electron microscopy (TEM), the formed metallic Cu NPs are well dispersed on the AC and the average size of NPs is 31.2 ± 3.2 nm as shown in Figure 1c, which is consistent with XRD result. In high-resolution TEM (HRTEM) images (Figure 1d), the characteristic spacing of 0.208 nm agrees well with the Cu (111) crystallographic planes, indicating the main component is metallic Cu in the 15 wt%-Cu/AC-600 catalyst.

In the characterization of catalytic properties, the obtained 15 wt%-Cu/AC-600 catalyst displays 99.9% vanillin conversion and 93.2% MMP selectivity in vanillin HDO (**Table 1**, Entry 1) under 120 °C, 2.0 MPa H_2 pressure within 5 h. By contrast, the HDO reaction does not proceed without catalyst (Table 1,

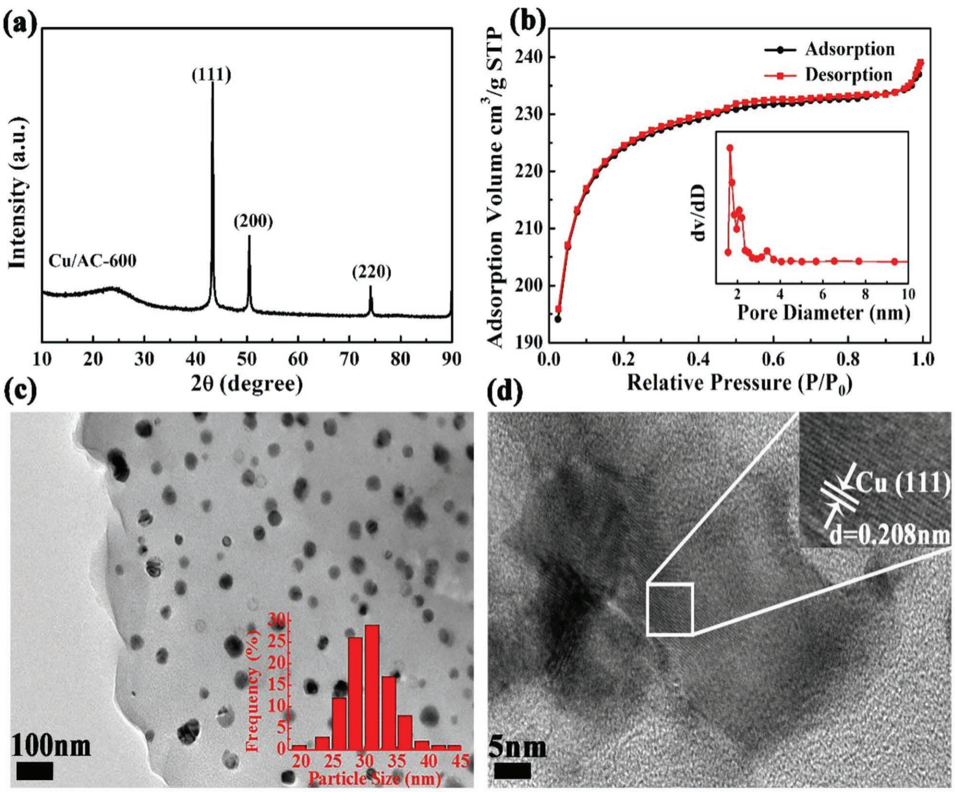

Figure 1. The characterization of 15 wt%-Cu/AC-600 catalyst. a) X-ray diffraction patterns, b) nitrogen adsorption–desorption isotherm and DFT pore size distributions, c) TEM image and the corresponding size distribution plot of Cu NPs (inset), and d) the HRTEM image.

Entry 2) or active metal (Table 1, Entry 3) under the identical reaction condition. In order to determine the active sites of Cu-based catalyst in the HDO of vanillin to MMP, the 15 wt%-Cu/AC-600 catalyst was further treated in air atmosphere at 200 °C. The obtained sample (15 wt%-Cu/AC-air-200) is mainly composed of copper oxide, as shown in Figure S1 (Supporting Information), and displays no activity in HDO of vanillin (Table 1, Entry 4), suggesting that the active sites are metallic copper rather than copper oxide. On this base, we also further reduced the 15 wt%-Cu/AC-air-200 catalyst in a reducing gas (H_2) at 300 °C. With reduction time prolonging, copper oxides are progressively reduced to metallic copper, as shown in Figure S1 of the Supporting Information (15 wt%-Cu/AC-reduced-1h, 15 wt%-Cu/AC-reduced-3h and 15 wt%-Cu/AC-reduced-6h in Supporting Information). Meanwhile, vanillin conversion and MMP selectivity gradually recover and are highly correlated with the reduction extent, as shown in Table S1 (Supporting Information). After 6 h reduction, the sample are mainly composed of metallic copper and displays 99.0% conversion and 90.7% selectivity, which are similar with the 15 wt%-Cu/AC-600 catalyst (99.9% conversion and 93.2% selectivity). Therefore, we deduce that the active sites of the 15 wt%-Cu/AC-600 catalyst are metallic Cu in HDO of vanillin. In view of the catalytic HDO performances (reaction conditions, conversion, selectivity, and TOF), the 15 wt%-Cu/AC-600 catalyst can be comparable with most reported high-performance HDO catalysts, including noble metal-based catalysts (Table S2, Supporting Information).

Table 1. The catalytic performance in HDO of vanillin.

	Catalyst[a)]	Mass [g]	Conversion [%]	Selectivity [%]	
				MMP	HMP
1	15 wt%-Cu/AC-600	0.03	99.9	93.2	6.8
2	–	–	–	–	–
3	AC	0.03	–	–	–
4	15 wt%-Cu/AC-air-200	0.03	–	–	–

[a)] Reaction conditions: vanillin (0.5 mmol), water (10 mL), P(H_2) = 2.0 MPa. Reaction temperature, 120 °C; reaction time, 5 h.

2.2. Aqueous-Phase HDO of Vanillin

A series of catalytic and characterization tests were conducted to experimentally investigate the influence of key parameters on activity of supported Cu catalysts, including carbothermal temperature, Cu loading amount, as well as some reaction variables.

2.2.1. Effect of Synthesis Parameters on Activity in HDO of Vanillin

Firstly, we prepared a series of 15 wt%-Cu/AC samples, which are derived from different carbothermal temperature (400–700 °C). In these samples, the actual Cu contents are basically same (14.4–14.8 wt% by inductively coupled plasma (ICP) analysis, Table S3 (Supporting Information)), and are consistent with the addition of precursors, suggesting the carbothermal temperature would not affect the Cu content. Consequently, we conducted the catalytic performance of these samples in aqueous-phase catalytic HDO of vanillin to MMP under a mild condition of 120 °C, 2.0 MPa H_2 within 5 h. **Figure 2** shows the correlations between carbothermal temperature and catalytic performance for 15 wt%-Cu/AC catalysts. As shown in Figure 2a, vanillin conversion raises from 29.4% to 93.2% with the carbothermal temperature of 15 wt%-Cu/AC catalyst increasing from 400 to 500 °C. And then near-quantitative vanillin conversion and 93.2% MMP selectivity are achieved when the carbothermal temperature increased to 600 °C. Meanwhile, as shown in Figure 2b, the copper phases are mainly composed of copper oxide at low carbothermal temperature of 400 °C, in which the diffraction peaks at 35.5° and 38.7° can be attributed to (002) and (111) planes of CuO (JCPDS 00-005-0661), and the peaks at 29.6°, 36.4°, 61.4°, 73.6°, 77.4° can be indexed to (110), (111), (220), (311), (222) planes of Cu_2O (JCPDS 01-078-2076). It could be seen clearly that the intensity of copper oxide phases gradually decreases with the carbothermal temperature increasing from 400 to 600 °C, and meanwhile the metallic copper becomes the main phase. This is mainly due to the reduction of copper precursor by AC followed as $CuO \rightarrow Cu_2O \rightarrow Cu$, which is strongly associated with temperature in carbothermal process. Meanwhile, the reacted AC is converted to carbon monoxide (CO) and sometimes carbon dioxide (CO_2) to form cavity on the surface of AC. Therefore, the values of S_{BET} increases from 769 $m^2\ g^{-1}$ (at 400 °C) to 840 $m^2\ g^{-1}$ (at 700 °C) due to the formation of more cavity on the surface of support by the stronger interaction between AC and Cu precursor with carbothermal temperature increase (Table S3 and Figure S2, Supporting Information). However, the activity of 15 wt%-Cu/AC catalyst is not directly proportional to the surface area because too high carbothermal temperature would induce NPs agglomeration that could be proved by TEM analysis. Hence, we further detected the morphologies and metal dispersions of 15 wt%-Cu/AC catalysts obtained at different temperatures (400, 500, 700 °C). As shown in Figures 1c and 2c, it can be seen clearly that the NPs are well dispersed on the AC substrate when the carbothermal temperature in the range of 400–600 °C, and the sizes of NPs are about 18.3 ± 2.7 nm at 400 °C, 27.8 ± 3.9 nm at 500 °C,

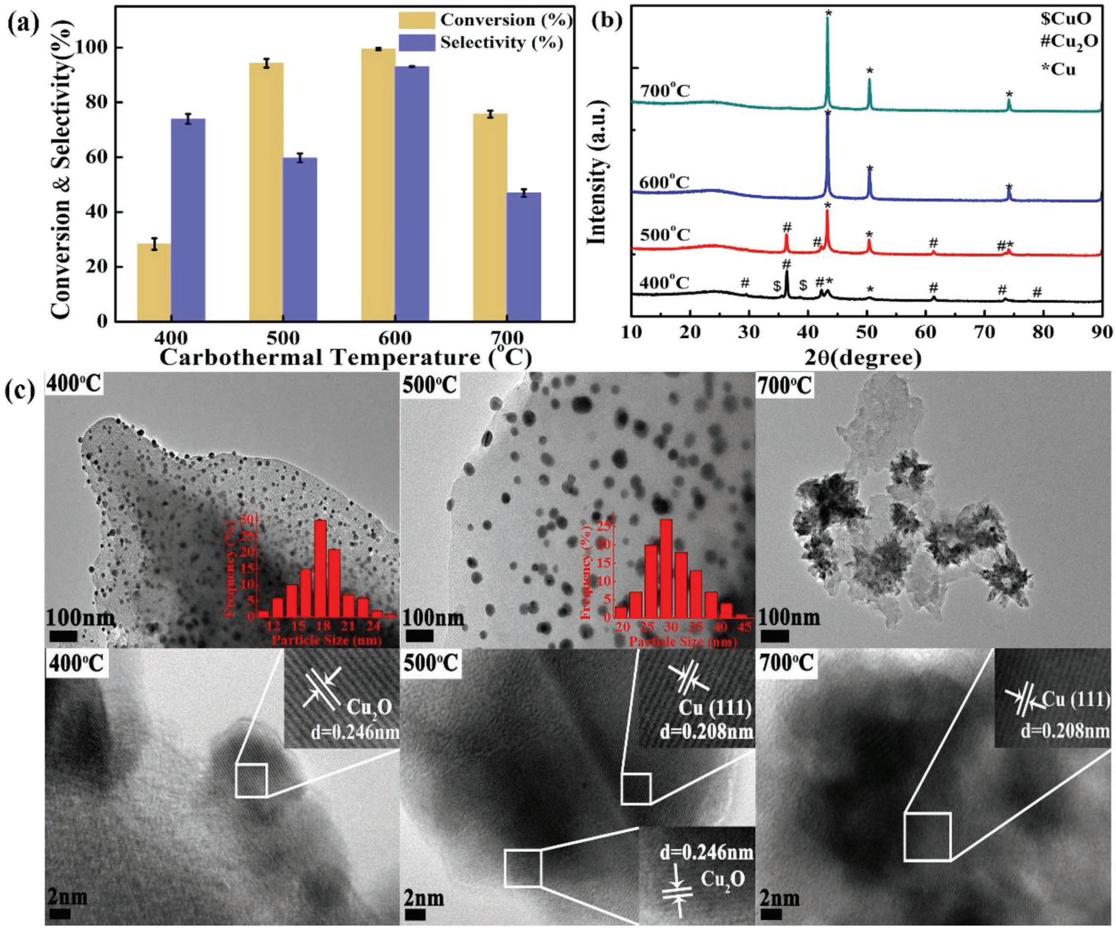

Figure 2. The structure–activity relationship under different carbothermal temperature. a) Catalytic activity in HDO of vanillin and b) XRD patterns of 15 wt%-Cu/AC catalysts obtained under 400, 500, 600, and 700 °C, c) TEM image of 15 wt%-Cu/AC catalysts (inset is the corresponding size distribution plot of Cu NPs) and their corresponding HRTEM at 400, 500, and 700 °C, respectively.

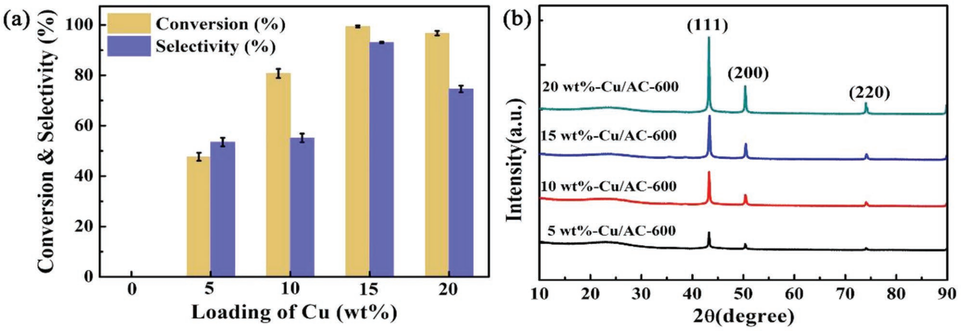

Figure 3. a) The catalytic performance of Cu/AC-600 catalyst with different loading amount of Cu. (Reaction conditions: 0.5 mmol vanillin, 10 mL water, 30 mg catalyst, 2.0 MPa H_2 pressure, 120 °C reaction temperature, 5 h reaction time.) b) XRD diffraction patterns of Cu/AC-600 catalysts with different Cu contents calcined at 600 °C in N_2 for 2 h.

and 31.2 ± 3.2 nm at 600 °C. These NPs are proved again as copper oxide (CuO and/or Cu_2O) at low carbothermal temperature of 400 and 500 °C, and metallic Cu NPs are obtained at carbothermal temperature of 600 °C, which were further examined by HRTEM images. With the carbothermal temperature increasing to 700 °C, although the NPs are displayed in the form of metallic Cu particles, a serious agglomeration of NPs occurs on the surface of support, which would greatly reduce the activity in HDO of vanillin. Combining the results of Figure 1, Table 1, and Figure 2, therefore, we deduce the metallic Cu is the active sites in HDO of vanillin, which is consistent with previous reports.[28,33,36]

In addition of carbothermal temperature, the Cu loading amount also has a great influence on the catalytic activity of Cu/AC-600 catalyst. Therefore, we prepared series of Cu/AC-600 catalyst with different Cu loading amount, and tested their catalytic activity in aqueous-phase HDO of vanillin under a mild condition of 120 °C, 2.0 MPa H_2 and 5 h. As shown in **Figure 3**a, the reaction of vanillin HDO cannot occur in the absence of metallic Cu. Then, vanillin conversion increases to 49.1% by using 5 wt%-Cu/AC-600 catalyst, suggesting metallic Cu is the essential element for transforming vanillin. The activity almost doubles as Cu loading amount increasing from 5 wt% to 10 wt%, indicating the metallic Cu NPs is participated effectively in HDO reaction. And then, full vanillin conversion is obtained when Cu loading amount is 15 wt%, which also gives highest MMP selectivity (93.2%). The XRD patterns and TEM images of Cu/AC-600 catalysts with different Cu loading have been displayed in Figure 3b and Figure S3 (Supporting Information). The XRD pattern of metallic Cu shows higher and sharper intensity with the increase of Cu loading due to the formation of more metallic Cu (Figure 3b), and the size of Cu NPs is not obviously affected by Cu loading except the 20 wt% system (Figure S3a–c, Supporting Information). These results further indicate clearly the metallic Cu can greatly enhance the activity and selectivity of catalytic HDO of vanillin. However, the catalytic activity of Cu/AC catalyst is reduced when the Cu loading increasing from 15 wt% to 20 wt% probably due to the agglomeration of metallic Cu at high loading amount (Figure S3d, Supporting Information). In view of these results, 15 wt% loading amount of Cu in the Cu/AC catalyst can give an optimal catalytic efficiency in aqueous-phase HDO of vanillin to MMP.

2.2.2. Optimization of Catalytic System and Reaction Pathway in HDO of Vanillin

The influence of the reaction temperature, time, and H_2 pressure were investigated to put forward the possible reaction pathway of vanillin over the 15 wt%-Cu/AC-600 catalyst, and the corresponding results were presented in **Figure 4** and Figure S4 (Supporting Information). First, the reaction behavior of vanillin HDO varying with reaction temperature over 15 wt%-Cu/AC-600 catalyst was depicted in Figure 4a and Figure S4a (Supporting Information). Vanillin conversion is enhanced evidently from 24.6% to 97.6% as reaction temperature increasing from 70 to 90 °C and further elevates up to

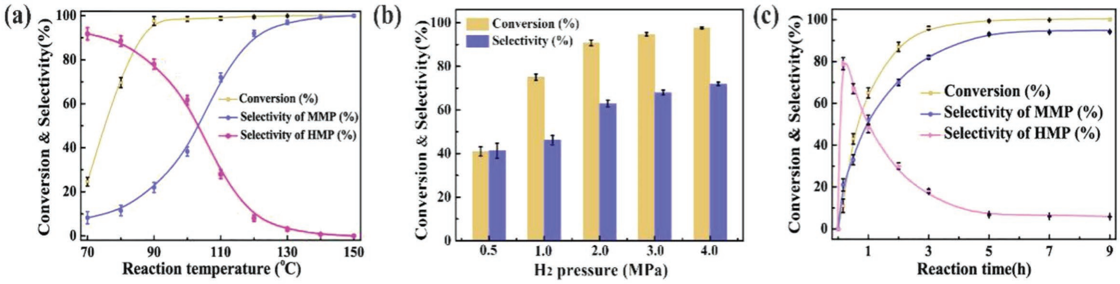

Figure 4. Effect of reaction conditions on the HDO of vanillin over 15 wt%-Cu/AC-600 catalyst (0.5 mmol vanillin, 10 mL water, 30 mg catalyst). a) Effect of reaction temperature at 2.0 MPa H_2 pressure for 5 h. b) Effect of H_2 pressure at 120 °C for 3 h. c) Product distributions as functions of time at 120 °C and 2.0 MPa H_2 pressure.

99.9% at 120 °C. Furthermore, the reaction temperature has a great influence on product distribution. At the reaction temperature lower than 100 °C, vanillin is mainly converted into HMP by the hydrogenation of C=O group of vanillin with low MMP selectivity. When the temperature increased from 70 to 120 °C, MMP selectivity upgrades from 9.7% to 93.2%, and then gradually approaches up to 99.5% as temperature further elevated to 150 °C because the C—O bond is activated as the temperature increases. As a result the hydrogenolysis of C—O is enhanced to generate the finally product of MMP.[22] On these basis, a plot of $\ln(C_{VA}/C_{VA,0})$ versus reaction time is depicted at different temperatures (Figure S5, Supporting Information). It is found that HDO of vanillin follows pseudo-first order kinetics. The values of k at various temperatures were calculated from the slope of the linear part of each plot in Figure S5a of the Supporting Information to determine the activation energy (E_a). Figure S5b of the Supporting Information shows the linear fitting of $\ln k$ and $1/T$. The apparent E_a could be calculated from the Arrhenius equation: $\ln k = \ln A - E_a/RT$, where $\ln A$ is the intercept of the line and R is the gas constant. Consequently, the calculated E_a value is ≈45.7 ± 1.9 kJ mol^{-1}, indicating the 15 wt%-Cu/AC-600 catalyst has high activity in the HDO of vanillin. Besides reaction temperature, the participation amounts of H_2 would also influence the catalytic activity in HDO of vanillin. The effect of H_2 pressure was investigated by varying in the range of 0.5–4.0 MPa (Figure 4b; Figure S4b, Supporting Information). Vanillin conversion is 39.8% at 0.5 MPa H_2 pressure, and then it reachs to 76.7% and 94.1% when the H_2 pressure increased to 1.0 and 2.0 MPa, respectively. Complete vanillin conversion is obtained when the pressure further increased to 4.0 MPa. Furthermore, MMP selectivity is also adjusted by the H_2 pressure especially in the range of 0.5–2.0 MPa. The upgraded activity of 15 wt%-Cu/AC-600 catalyst could be attributed to improvement of the dissolved H_2 with H_2 pressure increase. Considering catalytic efficiency, economy and energy consumption, the H_2 pressure at the favorable temperature 120 °C is 2.0 MPa for aqueous-phase HDO of vanillin.

To further prove the reaction pathway, the distribution of products as a function of reaction time were tracked and analyzed over the 15 wt%-Cu/AC-600 catalyst in aqueous-phase HDO of vanillin. Before studying the effect of reaction time, the impact of heating stage on reaction results had been eliminated as shown in Table S4 (Supporting Information), which shows vanillin conversion is lower than 2.5% in the end of heating indicating the reaction hardly takes place in the heating stage and would not affect the catalytic results. As can be seen in Figure 4c and Figure S4c (Supporting Information), the reaction is accompanied by a rapid increase in vanillin conversion with reaction time, and almost complete conversion can be obtained after 3 h reaction. In initial period, the reactant vanillin is mainly converted to HMP by hydrogenation of branched carbonyl group (C=O). And HMP selectivity gradually decreases, meanwhile the selectivity of target product MMP increases obviously with reaction progressing. The result is consistent with the reaction data in reaction temperature (Figure 4a), further indicating HMP is the intermediate to produce MMP. Therefore, the branched C=O group of vanillin is initially adsorbed and activated on the surface of metallic Cu and vanillin is converted to HMP quickly. The new formed C—O bond in HMP will rupture to further generate MMP. From these results, we can also draw a conclusion that the reaction rate of C—O bond cleavage is lower than the rate of C=O group hydrogenation.

We also investigated the dependence of chemical states of Cu species and carbothermal temperature in the 15 wt%-Cu/AC catalysts by X-ray photoelectron spectroscopy (XPS) analysis to verify the active sites in HDO of vanillin (**Figure 5**). The higher BE peak at ≈935 eV is assigned to Cu(II) in the spinel, accompanied by the characteristic Cu(II) shakeup satellite peaks (938–945 eV) (Figure 5a). The lower BE peak at ≈932 eV suggests the presence of Cu(I) or Cu(0) species.[29] The Cu species are mainly composed of Cu(II) (about 60.7% content) when the 15 wt%-Cu/AC sample was obtained at 400 °C. At high temperature, the reduction of AC is beneficial to the formation of low valence copper. At carbothermal temperature of 600 °C, the 15 wt%-Cu/AC is mainly composed of Cu(0) species, a small fraction of copper oxide appears, which is due to the oxidation on the surfaces of Cu (Figure 5b). Although the sample obtained at 700 °C is also mainly composed of Cu(0) species (Figure 5c), its lower activity in HDO of vanillin is attributed to serious agglomeration of NPs (Figure 2c). From the catalytic testing result (Figure 2a), we can deduce the metallic Cu is the active sites in Cu/AC catalyst. Interestingly, almost no changes were observed when comparing XPS spectrum of the as-synthesized and reused catalysts (Figure 5b,d), indicating excellent stability.

Generally, the transformation of a carbonyl group into a methyl group can proceed via three pathways: (1) direct hydrogenolysis of C=O bond, (2) hydrogenation of C=O bond and then dehydration, and (3) hydrogenation of C=O bond and then hydrogenolysis of C—O.[12,13,19] For the first pathway, direct hydrogenolysis of C=O bond would not generate HMP. However, this product was detected in our cases, especially displaying high selectivity at the initial period of HDO of vanillin, as can be seen in Figure 4a,c. Therefore, the first pathway can be excluded. The second and third pathway both would produce the intermediate HMP by hydrogenation of C=O bond. When analysis the chemical structure formula of HMP, it can deduce that the dehydration will not take place because the adjacent carbon of C-OH group has no H atom in the molecular, indicating the HDO of vanillin is unlikely to pass through the second way.[19] Therefore, we conject that vanillin is first transformed into HMP by the hydrogenation of branched C=O group on the active sites of Cu(0) species, and then the generated C—O bond will break by the hydrogenolysis of C—O to generate the desired product of MMP, and the deduction lines up with the catalytic results. As such, the metallic Cu is the active site in HDO of vanillin and gives high selectivity to MMP. The adsorption of vanillin on Cu(111) gives a clear evidence that high MMP selectivity can be achieved by the as-synthesized 15 wt%-Cu/AC-600 catalyst (**Figure 6**), and the corresponding coordinates of relaxed geometries had been listed in the Supporting Information. Vanillin contains three O atoms, one in the carbonyl and the other two are located in methoxyl and phenol hydroxyl. The adsorption energy and distance between the O atoms and Cu(111) can reflect the adsorption properties of functional groups on Cu(111) surface. Based on density function theory

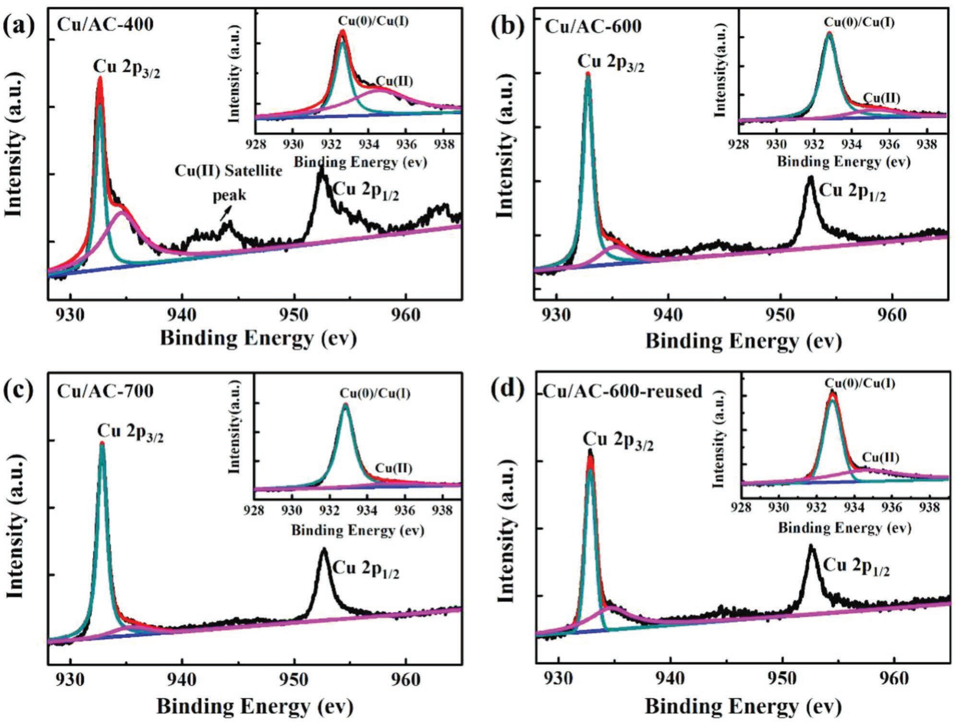

Figure 5. XPS spectrums of Cu/AC (15 wt%) catalysts. a) Cu/AC-400, b) Cu/AC-600, c) Cu/AC-700, and d) Cu/AC-600-reused.

(DFT) calculations, the carbonyl group (Figure 6a) gives the lowest adsorption energy (−39.6 ± 2.2 kJ mol^{-1}) and shortest distance between Cu(111) and O atom when compared with methoxyl (Figure 6b) and phenol hydroxyl groups (Figure 6c). Therefore, the 15 wt%-Cu/AC-600 catalyst can selectively adsorb carbonyl group on active sites resulting in activation and hydrogenation of carbonyl group. Consequently, vanillin is highly converted to MMP.

2.3. Organic-Phase THR of Vanillin over Cu/AC

2.3.1. Hydrogen Donor in THR of Vanillin

We had demonstrated that the 15 wt%-Cu/AC-600 catalyst has high activity in aqueous-phase HDO of vanillin at 70–150 °C. However, even though the temperature increased to 180 °C, almost no activity is observed without using H_2 (**Table 2**, Entry 1), indicating water cannot use as a hydrogen donor at this condition.[38] When, we added a bit of 2-propanol into the water (V_{water}:$V_{\text{2-propanol}}$ = 9:1), 3.5% vanillin can transform into MMP (Table 2, Entry 2), and the efficiency increases to 26.1% when the proportion of water and 2-propanol was 1:1 (Table 2, Entry 3). And near-quantitative vanillin conversion and 99.1% MMP selectivity can be obtained when the solvent water was replaced by 2-propanol (Table 2, Entry 4). These results demonstrates that the protic solvent of 2-propanol can replace molecular H_2 to provide active H, which can be used as solvent and hydrogen donor, simultaneously. In addition, similar to the HDO reaction, the THR reaction also do not proceed without catalyst (Table S5, Entry 1, Supporting Information) or active metal (Table S5, Entry 2, Supporting Information). Notably, even the use of 15 wt%Cu/AC-air-200, which is mainly composed of copper oxide, also displays no activity in THR of vanillin (Table S5, Entry 3, Supporting Information) under the identical reaction condition (Table S5, Supporting Information).

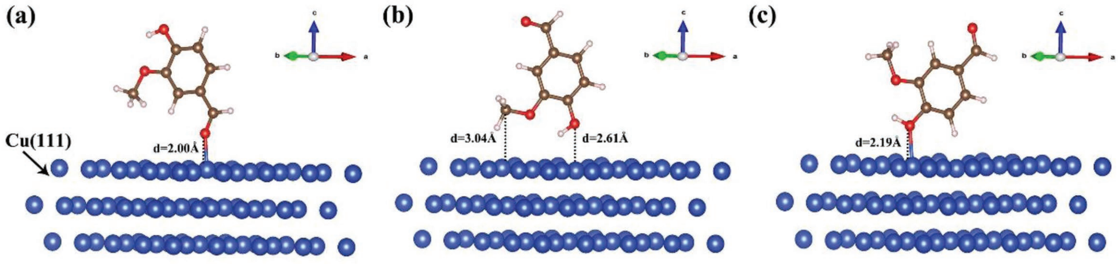

Figure 6. DFT Optimized geometries of oxygen functional groups in vanillin for adsorption configuration on Cu(111). a) C=O group, b) methoxyl group, and c) phenol hydroxyl group. Red, brown, and white spheres represent oxygen, carbon, and hydrogen atoms, respectively.

Table 2. The results of the solvent effect in THR of vanillin.

Entry[a)]	Solvent	Conversion [%]	MMP selectivity [%]
1	H_2O	–	–
2	V_{water}:$V_{2\text{-propanol}}$ = 9:1	3.5	99.9
3	V_{water}:$V_{2\text{-propanol}}$ = 1:1	26.1	99.7
4	2-propanol	99.8	99.1

[a)] Reaction conditions: vanillin, 0.5 mmol; solvent, 10 mL; 15 wt%-Cu/AC-600 catalyst, 30 mg (Cu loading amount was 15 wt%); reaction temperature, 180 °C; reaction time, 5 h.

Table 3. The results of the THR of vanillin with different alcohols.

Entry[a)]	Solvent	Conversion [%]	MMP selectivity [%]
1	H_2O	–	–
2	Methanol	17.3	74.4
3	Ethanol	73.2	98.5
4	n-propanol	88.6	95.1
5	n-butanol	84.1	93.3
6	2-propanol	99.8	99.1

[a)] Reaction conditions: vanillin, 0.5 mmol; solvent, 10 mL; 15 wt%-Cu/AC-600 catalyst, 30 mg (Cu loading amount was 15 wt%); reaction temperature, 180 °C; reaction time, 5 h.

A series of alcohols were also selected as hydrogen donors to study the effect of solvents in the catalytic THR of vanillin to MMP. The THR tests were examined within 5 h under 180 °C reaction temperature, and products are mainly composed of MMP (**Table 3**). When using primary alcohols as the solvent and hydrogen donors, vanillin conversion and MMP selectivity are proportional to the chain length from the C1 to C4: n-butanol ≈ n-propanol > ethanol > methanol. When using 2-propanol instead of primary alcohols, vanillin conversion and MMP selectivity are almost close to 100% indicating the vanillin can be completely converted into MMP under this circumstance. Moreover, the condensation reaction between vanillin and alcohol is also more likely to take place by using primary alcohols than that of 2-propanol.[39,40] Therefore, 2-propanol is one of the optimal candidates as the solvent and hydrogen donors in the process of vanillin THR to MMP over the 15 wt%-Cu/AC-600 catalyst.

2.3.2. Optimization of Catalytic System and Reaction Pathway on THR of Vanillin

The influence of reaction temperature on the catalytic THR of vanillin over the 15 wt%-Cu/AC-600 catalyst was investigated and the result is shown in **Figure 7**a. The vanillin THR is hardly taken place when the reaction temperature lower than 170 °C. When the temperature reached 180 °C, the activity of THR is suddenly woken up and almost all of vanillin is transformed into MMP under this reaction condition. One of the most important steps is to generate active hydrogen from protic solvent by dehydrogenation. For example, the dehydrogenation of 2-propanol will generate acetone and hydrogen.[41] At low reaction temperature, it is hard to take place dehydrogenation of protic solvent to release hydrogen, which will further restrict vanillin THR. To prove this, we evaluated the catalytic activity of 15 wt%-Cu/AC-600 catalyst in dehydrogenation of 2-propanol under reaction temperatures of 150–180 °C (Figure S6, Supporting Information). Only trace amount of acetone was detected at 150 °C indicating dehydrogenation is hardly taken place at low reaction temperature, and the dehydrogenation is greatly enhanced as the temperature elevating to 180 °C. The result is consistent with Figure 7a. Therefore, it is important to provide sufficient energy to drive active hydrogen releasing from protic solvent and it will be the rate controlling step to THR.

To further investigate the reaction pathway, the distribution of products as a function of reaction times was tracked over the 15 wt%-Cu/AC-600 catalyst in THR of vanillin, as shown in Figure 7b. Interestingly, the converted reactant is almost completely transformed into MMP in the THR of vanillin under 180 °C in the overall reaction, which is quite different from HDO of vanillin. MMP selectivity can reach 90.1% at the initial reaction stage, and then up to 99.1% as the reaction time prolonging to 5 h. Therefore, the pathway in THR of vanillin is probably distinguished with the reaction route in HDO of vanillin. For the possible reaction route, active H is first generated from dehydrogenation of 2-propanol on the active metallic Cu, and then it contacts with vanillin on the surface of catalyst

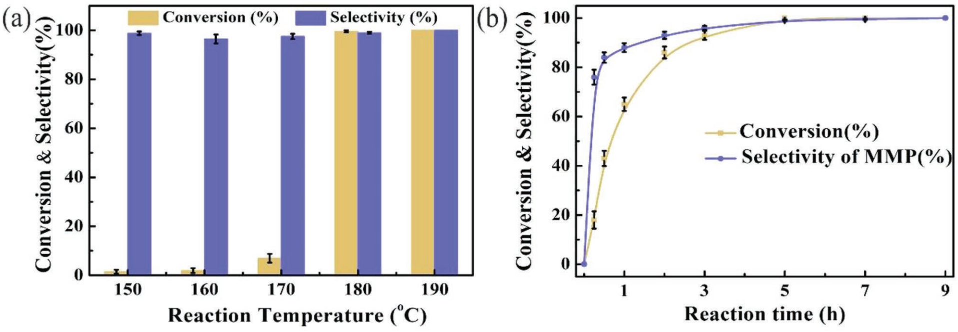

Figure 7. Effect of reaction temperature and time on the vanillin THR over 15 wt%-Cu/AC-600 catalyst (reaction conditions: 0.5 mmol vanillin, 30 mg catalyst, 10 mL 2-propanol). a) Effect of reaction temperature (reaction time 5 h). b) Product distributions as functions of time (reaction temperature 180 °C).

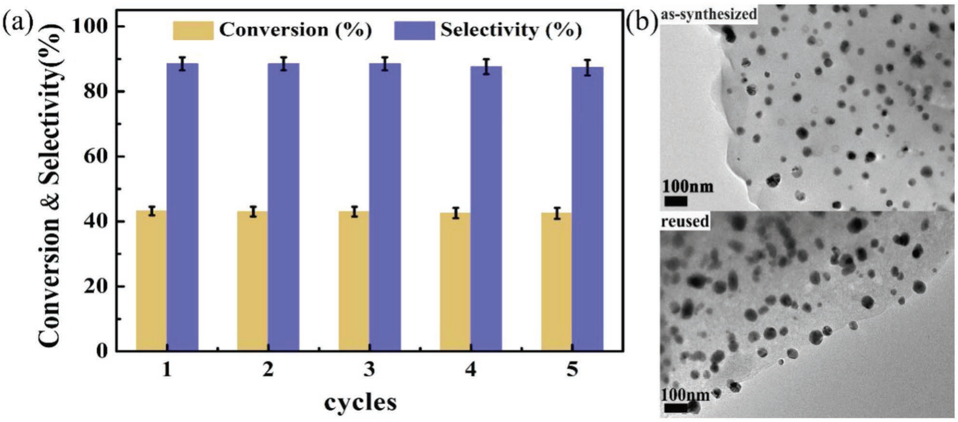

Figure 8. a) Recycling performance for the conversion of vanillin and selectivity to MMP after 5 cycles over the 15 wt%-Cu/AC-600 catalyst. b) A representative TEM image of the as-synthesized and reused 15 wt%-Cu/AC-600 catalyst after five runs, respectively.

to directly take place hydrogenolysis reaction to form the target product MMP. These results reveal that the15 wt%-Cu/AC-600catalyst not only has high catalytic performance in HDO of vanillin, but also demonstrated excellent activity in THR with 2-propanol as the hydrogen donor for transforming vanillin into MMP. So far, the studies of carbonyl compounds THR, like vanillin or furfural, are mostly focused on the noble metal catalysts. Our study also proved that the Cu-based catalyst has an outstanding catalytic performance in carbonyl compounds THR.[38]

2.3.3. Catalyst Reusability

The reusability of 15 wt%-Cu/AC-600catalyst had also been investigated in THR of vanillin (**Figure 8**). The catalyst is quite stable and the conversion and selectivity do not change for reusing 5 cycles (Figure 8a). The TEM images of the as-synthesized and reused catalytic reaction show that the morphology of the15 wt%-Cu/AC-600 catalyst do not change after 5 cycle reaction, and no catalyst loss or agglomeration occurs (Figure 8b). Furthermore, the excellent stability of 15 wt%-Cu/AC-600 catalyst could also be testified by XRD analysis of as-synthesized and used catalyst, in which there are almost no changes in the XRD diffraction peaks (Figure S7, Supporting Information). Besides, according to ICP analysis, the Cu contents in the as-synthesized and reused 15 wt%-Cu/AC-600 are 14.5 wt% and 14.3 wt%, respectively, suggesting that no leaching of Cu in reaction process.

3. Conclusion

In summary, we show that Cu/AC catalyst, which was prepared by one-pot carbothermal method, not only has efficient catalytic performance in aqueous-phase HDO of vanillin, but also exhibits high activity in organic-phase THR of vanillin. The 15 wt%-Cu/AC-600 catalyst obtained at 600 °C displays uniform dispersed metallic Cu NPs which acts as active sites in the two reaction processes. In aqueous-phase HDO of vanillin, the desired product MMP is generated through hydrogenolysis of the intermediate HMP, which is formed by hydrogenation of carbonyl group in vanillin. Near-quantitative vanillin conversion and 93.2% MMP selectivity are achieved within 5 h under reaction temperature 120 °C and 2.0 MPa H_2 pressure, which is one of the optimal conditions in identical reaction based on catalytic and energy efficiency. When we applied the 15 wt%-Cu/AC-600 to THR of vanillin, it also presents superior catalytic performance, in which 99.8% vanillin conversion and 99.1% MMP selectivity are obtained within 5 h under 180 °C by using 2-propanol as the solvent and hydrogen donor. And the cycle test suggests the prepared catalyst has good stability. In general, the facilely prepared Cu/AC by one-pot carbothermal method provides an alternative to noble-metal (Pt, Pd, Ru, and Rh) catalysts in the conversion of vanillin toward MMP in practical application.

4. Experimental Section

Chemicals and Materials: All reagents with AR purity (analytical reagent grade) were used as received without further purification. Cupric nitrate ($Cu(NO_3)_2{\cdot}3H_2O$), methanol, anhydrous ethanol, 2-propanol, and 2-butanol were purchased from the Sinopharm Chemical Reagent. The n-propanol, n-butanol, ethyl acetate, vanillin, and activated carbon (AC) were purchased from Aladdin reagent (Shanghai) Co. Ltd. Deionized water with a resistance larger than 18.2 MΩ used throughout the experiments.

Preparation of Catalysts: The supported Cu catalyst was synthesized by carbothermal reduction method, in which Cu precursor was calcined to copper oxide and then reduced to metallic Cu by AC under a certain temperature. Typically, 0.57 g $Cu(NO_3)_2{\cdot}3H_2O$ was dissolved in 1 mL deionized water. Then 1 g AC was added into the above solution. After the solution completely impregnated into the AC, the sample was dried under vacuum at 60 °C for 24 h. The dried sample was then treated in N_2 at 600 °C for 2 h at a heating rate of 5 °C min^{-1} to obtain the 15 wt%-Cu/AC-600 catalyst. Correspondingly, the catalysts derived at other carbothermal temperature (400, 500, and 700 °C) were also prepared and compared with 15 wt%-Cu/AC-600.

Characterization of the Catalysts: The crystalline structures of the samples were identified by XRD analysis (Philips X' pert PRO) using Ni-filtered monochromatic Cu Kα radiation at 40 kV and 40 mA. The morphology and structure of the products were characterized using TEM (JEOL-2010, 200 kV) with an energy dispersive X-ray spectrometer (EDS Oxford, Link ISIS). The specific surface areas and the pore distributions of the samples were calculated by nitrogen adsorption (Micrometrics

ASAP 2020M) at –196 °C using the BET equation. Quantitative determination of the metal ion content (Cu) was performed by ICP or inductively coupled plasma mass spectrometry (ICP-MS). XPS analysis was performed on an ESCALAB 250 X-ray photoelectron spectrometer (Thermo, USA) equipped with Al $K\alpha_{1,2}$ monochromatized radiation at 1486.6 eV X-ray source.

HDO of Vanillin: The reactions were carried out in a 25 mL stainless steel autoclave equipped with a magnetic stirrer. Certain amount of Cu/AC catalyst (30 mg) was introduced into the reactor together with 0.5 mmol of vanillin (reagent) in 10 mL water (solvent). When the reactor had been pressurized with H_2 to a relevant pressure (0.5–4.0 MPa), the reactor was heated to a setting temperature (70–170 °C) and maintained at this temperature for a setting reaction time with 600 rpm stirring. After reaction, the reactor was cooled down quickly. The product mixture and used catalyst were separated by centrifugation.

THR of Vanillin: N_2 gas was used to replace H_2 gas and the solvent of water was replaced by some protic solvents. The other procedure of THR of vanillin was similar with HDO of vanillin.

Product Analysis: In HDO reaction, the liquid products were extracted by ethylacetate (3 mL/time × 3 time) and the organic phase was collected. In THR reaction, the liquid products were collected by centrifugation. The samples were identified by gas chromatography-mass spectrometry (GC-MS, Thermo Fisher Scientific-TXQ Quntum XLS), and were quantitatively analyzed by GC (Shimadzu, GC-2010 Plus), equipped with FID and a KB-WAX capillary column (30 m × 0.25 mm × 0.25 µm, Kromat Corporation, USA) using n-octanol as an internal standard.

Vanillin conversion, MMP selectivity and mass balance (based on carbon) were calculated according to Equations (1–3)

$$\text{Conversion}(\%) = \frac{C_{\mathrm{VA},0} - C_{\mathrm{VA}}}{C_{\mathrm{VA},0}} \times 100\% = \left(1 - \frac{C_{\mathrm{oc}}}{C_{\mathrm{VA},0}} \times f_{\mathrm{VA}} \times \frac{A_{\mathrm{VA}}}{A_{\mathrm{OC}}}\right) \times 100\% \tag{1}$$

$$\text{MMP selectivity}(\%) = \frac{C_{MMP}}{\sum C_i} \times 100\% = \left(\frac{C_{\mathrm{oc}} \times f_{\mathrm{MMP}} \times \frac{A_{\mathrm{MMP}}}{A_{\mathrm{OC}}}}{\sum C_{\mathrm{oc}} \times f_i \times \frac{A_i}{A_{\mathrm{OC}}}} \right) \times 100\% \tag{2}$$

$$\text{Mass balance} = \frac{\sum C_i + C_{\mathrm{VA}}}{C_{\mathrm{VA},0}} \times 100\% \tag{3}$$

where, $C_{\mathrm{VA},0}$ is the initial concentration of vanillin, C_{VA} is the concentration of vanillin in mixed product after reaction, and C_{oc} is the concentration of n-octanol. A_{VA} and A_{OC} represent the peak areas of vanillin and n-octanol detected by GC-FID, and the f_{VA} is the correction factor between vanillin and n-octanol. C_{MMP} is the concentration of MMP in product and C_i is the concentration of product i (including MMP, HMP and trace amount other products), A_{MMP} and A_i are attributed to the peak areas of MMP and product i in GC-FID chromatogram, and f_i is the correction factor between product i and n-octanol. The mass balance (based on carbon) was checked in every experimental run and detected to be higher than 98%.

Computational Methods: All the calculations were performed within the framework of DFT, using the Vienna Ab initio Simulation Package with Perdew–Burke–Ernzerhof generalized gradient approximation function. The projector augmented wave method were used to describe the inert core electrons. The structures were relaxed until the total energy changes within 1×10^{-4} eV per atom and the Hellmann–Feynman force on each atomic site was less than 0.05 eV Å^{-1}, with a 300 eV cutoff energy. Cu(1 1 1) slab model was constructed with three metal layers and 20 Å vacuum space. The Gamma(Γ)-point Monkhorst–Pack sampling was used for the Brillouin zone. In all the calculations, the top two layers of the surfaces were allowed to relax together with adsorbates, while the bottom one layer was keep fixed to present the bulk properties. The adsorption energy, E_{ads}, is given by the following equation: $E_{\mathrm{ads}} = E_{\mathrm{slab/ads}} - E_{\mathrm{molecule}}$.

Supporting Information

Supporting Information is available from the Wiley Online Library or from the author.

Acknowledgements

This work was financially supported by the National Natural Science Foundation of China (Grant Nos. 51432009, 51502297, and 51372248), and Instrument Developing Project of the Chinese Academy of Sciences (Grant No. yz201421).

Conflict of Interest

The authors declare no conflict of interest.

Keywords

carbothermal, copper, hydrodeoxygenation, transfer-hydrogenation, vanillin

Received: May 22, 2018
Revised: June 25, 2018

[1] H. H. Khoo, P. N. Sharratt, P. Das, R. K. Balasubramanian, P. K. Naraharisetti, S. Shaik, *Bioresour. Technol.* **2011**, *102*, 5800.
[2] L. Petrus, M. A. Noordermeer, *Green Chem.* **2006**, *8*, 861.
[3] T. H. Parsell, B. C. Owen, I. Klein, T. M. Jarrell, C. L. Marcum, L. J. Haupert, L. M. Amundson, H. I. Kenttamaa, F. Ribeiro, J. T. Miller, M. M. Abu-Omar, *Chem. Sci.* **2013**, *4*, 806.
[4] G. W. Huber, S. Iborra, A. Corma, *Chem. Rev.* **2006**, *106*, 4044.
[5] H. Zacher, M. V. Olarte, D. M. Santosa, D. C. Elliott, S. B. Jones, *Green Chem.* **2014**, *16*, 491.
[6] J. Yang, C. L. Williams, A. Ramasubramaniam, P. J. Dauenhauer, *Green Chem.* **2014**, *16*, 675.
[7] J. N. Chheda, G. W. Huber, J. A. Dumesic, *Angew. Chem., Int. Ed.* **2007**, *46*, 7164.
[8] M. Fache, B. Boutevin, S. Caillol, *ACS Sustainable Chem. Eng.* **2016**, *4*, 35.
[9] X. Yang, Y. Liang, X. Zhao, Y. Song, L. Hu, X. Wang, *RSC Adv.* **2014**, *4*, 31932.
[10] L Zhu, Y Jiang, J Zheng, N Zhang, C Yu, Y Li, CW Pao, JL Chen, C Jin, JF Lee, CJ Zhong, B Chen, *Small* **2015**, *11*, 4385.
[11] X. Yang, Y. Liang, Y. Cheng, W. Song, X. Wang, Z. Wang, *Catal. Commun.* **2014**, *47*, 28.
[12] M Wan, X Zhang, M Li, B Chen, J Yin, H Jin, L Lin, C Chen, N Zhang, *Small* **2017**, *13*, 1701395.
[13] S. Crossley, J. Faria, M. Shen, D. E. Resasco, *Science* **2010**, *327*, 68.
[14] Z. Lv, Q. Sun, X. Meng, F. S. Xiao, *J. Mater. Chem. A* **2013**, *1*, 8630.
[15] F. M. Zhang, Y. Jin, Y. H. Fu, Y. J. Zhong, W. D. Zhu, A. A. Ibrahim, M. S. El-Shall, *J. Mater. Chem. A* **2015**, *3*, 17008.
[16] Y. Z. Chen, G. Cai, Y. Wang, Q. Xu, S. H. Yu, H. L. Jiang, *Green Chem.* **2016**, *18*, 1212.
[17] A. K. Singh, S. Jang, J. Y. Kim, S. Sharma, K. C. Basavaraju, D. P. Kim, *ACS Catal.* **2015**, *5*, 6964.
[18] A. Aijaz, Q. L. Zhu, N. Tsumori, T. Akitaa, Q. Xu, *Chem. Commun.* **2015**, *51*, 2577.
[19] X. Xu, Y. Li, Y. Gong, P. Zhang, H. Li, Y. Wang, *J. Am. Chem. Soc.* **2012**, *134*, 16987.

[20] S. Verma, R. B. N. Baig, M. N. Nadagoudab, R. S. Varma, *Green Chem.* **2016**, *18*, 1327.
[21] A. A. Ibrahim, A. Lin, F. M. Zhang, K. M. AbouZeid, M. S. El-Shall, *ChemCatChem.* **2017**, *9*, 469.
[22] F. M. Zhang, S. Zheng, Q. Xiao, Y. J. Zhong, W. D. Zhu, M. S. El-Shall, *Green Chem.* **2016**, *18*, 2900.
[23] K. Yan, J. Y. Liao, X. Wu, X. M. Xie, *RSC Adv.* **2013**, *3*, 3853.
[24] B. J. ONeill, D. H. K. Jackson, A. J. Crisci, C. A. Farberow, F. Y. Shi, P. M. Voyles, *Angew. Chem.* **2013**, *125*, 14053.
[25] R. F. Nie, H. Yang, H. F. Zhang, X. L. Yu, X. H. Lu, D. Zhou, Q. H. Xia, *Green Chem.* **2017**, *19*, 3126.
[26] G. L. Liu, A. W. Robertson, M. M. J. Li, W. C. H. Kuo, M. T. Darby, M. H. Muhieddine, Y. C. Lin, K. Suenaga, M. Stamatakis, J. H. Warner, S. C. E. Tsang, *Nat. Chem.* **2017**, *9*, 810.
[27] L. He, Y. Qin, H. Lou, P. Chen, *RSC Adv.* **2015**, *5*, 43141.
[28] S. Sitthisa, T. Sooknoi, Y. Ma, P. B. Balbuena, D. E. Resasco, *J. Catal.* **2011**, *277*, 1.
[29] P. Liu, E. J. M. Hensen, *J. Am. Chem. Soc.* **2013**, *135*, 14032.
[30] S. Nishimura, *Handbook of Heterogeneous Catalytic Hydrogenation for Organic Synthesis*, John Wiley & Sons, Inc, USA **2001**.
[31] X. Kong, L. Chen, *Catal. Commun.* **2014**, *57*, 45.
[32] M. M. Villaverde, N. M. Bertero, T. F. Garetto, A. J. Marchi, *Catal. Today* **2013**, *213*, 87.
[33] B. M. Nagaraja, V. S. Kumar, V. Shasikala, A. H. Padmasri, B. Sreedhar, B. D. Raju, *Catal. Commun.* **2003**, *4*, 287.
[34] S. Srivastava, N. Solanki, P. Mohanty, K. A. Shah, J. K. Parikh, A. K. Dalai, *Catal. Lett.* **2015**, *145*, 816.
[35] J. C. Ma, S. Liu, X. J. Kong, X. P. Fan, X. L. Yan, L. Chen, *Res. Chem. Intermed.* **2012**, *38*, 1341.
[36] S. Lomate, A. Sultana, T. Fujitani, *Catal. Sci. Technol.* **2017**, *7*, 3073.
[37] L. Petitjean, R. Gagne, E. S. Beach, D. Xiao, P. T. Anastas, *Green Chem.* **2016**, *18*, 150.
[38] R. F. Nie, X. L. Peng, H. F. Zhang, X. L. Yu, X. H. Lu, D. Zhou, *Catal. Sci. Technol.* **2017**, *7*, 627.
[39] M. J. Taylor, L. J. Durndell, M. A. Isaacs, C. M. A. Parlett, K. Wilson, A. F. Lee, *Appl. Catal., B* **2016**, *180*, 580.
[40] B. Chen, F. Li, Z. Huang, G. Yuan, *Appl. Catal., A* **2015**, *500*, 23.
[41] J. Lee, T. Ryu, S. Park, P. H. Lee, *J. Org. Chem.* **2012**, *77*, 4821.